ENHANCEMENT OF MANEUVERABILITY OF A POWER ASSIST OMNI-DIRECTIONAL WHEELCHAIR BY APPLICATION OF NEURO-FUZZY CONTROL

Kazuhiko Terashima and Juan Urbano
Department of Production Systems Engineering, Toyohashi University of Technology
Hibarigaoka 1-1, Toyohashi, 441-8580, Japan

Hideo Kitagawa
Department of Electronic Control Engineering, Gifu National College of Technology
Kamimakuwa, Motosu, Gifu, 501-0495, Japan

Keywords: Omni-directional wheelchair, power assistant, neuro-fuzzy systems, operability.

Abstract: A power assist system has been added to an Omni-directional Wheelchair (OMW) for helping attendants of handicapped people and elderly people, . With this addition it is possible for the attendants to deal with heavy loads, but there is a problem of operability when the attendants want to easily move OMW laterally or rotate around OMW's Gravity Center ***(CG)***. To solve the present problem, this paper provides a fuzzy reasoning method for estimating the navigation direction according to the force added by the attendants to the handgrips of the handle of OMW. A neuro-fuzzy system (ANFIS) is used for auto-tuning of the membership functions of the fuzzy system according to each attendant's characteristics, by using input data of attendants.

1 INTRODUCTION

In order to satisfy the demand for higher mobility, designers have created new driving concepts such as omni-directional movement which allows any combination of forward, sideways, and rotational movement, thus ensuring users much more freedom and safety in wide or narrow spaces. A variety of wheelchairs with different options and special add-on features have been developed to meet a wide range of needs (Wada and Asada, 1999)-(West and Asada, 1992).

In the author's laboratory, a holonomic Omni-directional Wheelchair (OMW) which can act as an autonomous (Kitagawa et al., 2002) or semi-autonomous (Kitagawa et al., 2001) omni-directional wheelchair has been developed.Comfort has been a subject of study in the case with and without the joystick (Kitagawa et al., 2002), (Terashima et al., 2004).

For handicapped people or elderly people that can use their arms freely, many power assisted wheelchairs have been developed such as (Seki et al., 2005), (FrankMobilitySystems, 2002), for example. However, it is necessary to consider that some elderly people or handicapped people can not use their arms because they are damaged or they are so weak. These people needs the help of an attendant. Considering this background, a power assist system that helps attendants to move a heavy load has been designed and developed in author's laboratory (Kitagawa et al., 2004). Application of power assist for supporting the attendant of an omni-directional wheelchair is one of a novel research. To the authors knowledge, no other report about this topic has appeared yet. However, there is some research about power system for omni-directional vehicles, but it is related to carts (Maeda et al., 2000), not to wheelchairs. Moreover, it still has some problems in rotation and in occupant's comfort since this system was developed for a food tray carry vehicle in a hospital.

However, there is a problem related to the operability of the OMW. Due to the application of the power assist system, operability of the OMW degrades, especially when the attendant tries to rotate in clockwise (CW), or counter-clockwise (CCW) direction around the center of gravity (***CG***) of the OMW.

It was impossible to find general rules that explained all cases, but a relationship was found between lateral and rotational movements. These relationships were used as the base for constructing a fuzzy reasoning system (MathWorks, 2002)-(Harris et al., 1993) that helped to improve the operability of the OMW.

Nevertheless, when the system was tested by dif-

Terashima K., Urbano J. and Kitagawa H. (2006).
ENHANCEMENT OF MANEUVERABILITY OF A POWER ASSIST OMNI-DIRECTIONAL WHEELCHAIR BY APPLICATION OF NEURO-FUZZY CONTROL.
In *Proceedings of the Third International Conference on Informatics in Control, Automation and Robotics*, pages 67-75
DOI: 10.5220/0001213700670075
Copyright © SciTePress

Figure 1: Omni-directional wheelchair (OMW).

ferent attendants, it was found that a complete satisfactory result was not obtained by every attendant. It is because each person has its own tendencies and the fuzzy inference system must be tuned to respond to them. Tuning of the fuzzy inference system by trial and error thus has been tried in (Kitagawa et al., 2004). However it is a time consuming and needs a lot of trials of the attendants, then these can become tired and bored.

Thus, a better tuning method, a method that allows tuning of the fuzzy inference system, is needed. It can be obtained by adding Neural Networks (NN) to the fuzzy inference system, obtaining what is known as a neuro-fuzzy system. There is a lot of research in this topic (Jang, 1993)-(Lin and Lee, 1991), being the basic difference the kind of NN that is used in combination with the fuzzy inference system.

Jang (Jang, 1993) developed ANFIS: Adaptive-Network-based Fuzzy Inference Systems, a neuro-fuzzy system in which the fuzzy inference system is tuned by using the input data of the system.

Hence, in this paper, a method for improving the operability of a power assist omni-directional wheelchair is presented.

2 OMNI-DIRECTIONAL WHEELCHAIR

A holonomic omni-directional wheelchair (OMW) using omni-wheels has been built, as is described in (Kitagawa et al., 2002)-(Kitagawa et al., 2001). Figure 1 shows an overview of the OMW.

The OMW is able to move in any arbitrary direction without changing the direction of the wheels. In this system, four omni-directional wheels are individually and simply driven by four motors. Each wheel has passively driven free rollers at their circumference. The wheel that rolls perpendicularly to the direction of movement does not stop its movement because of the passively driven free rollers. These wheels thus allow movement that is holonomic and omni-directional.

In semi-autonomous mode, a joystick is used as the input device. The OMW's direction of movement depends on the orientation of the joystick, while the speed of the OMW is proportional to the inclination of the joystick in the direction of movement. Moreover, eight ultrasonic sensors and eight PSD sensors are distributed around the OMW's base in order to acquire information regarding the environment.

The OMW is also equipped with a handle and a six-axis force sensor, as shown in Fig. 1, that allows the OMW's use in power-assist mode. The force that the attendant inputs to the grips of the handle is measured by this force sensor.

3 POWER ASSIST SYSTEM

3.1 Second Order Controller for Power Assist

When a first order controller is used for the transformation from force to velocity (Kitagawa et al., 2004), a big jerk (derivative of acceleration) appears if the input force changes suddenly. Jerk is considered as the factor that dominates the riding comfort. For the riding comfort's improvement, jerk must be decreased. A second order controller

$$G_i(s) = \frac{V_i(s)}{F_i(s)} = \frac{K(\omega_n)_i^2}{s^2 + 2\zeta_i(\omega_n)_i s + (\omega_n)_i^2}, \qquad (1)$$

is chosen as a power assist controller which can provide compatibility for both operability and riding comfort. Here, ζ is the attenuation factor. Even when the force added by attendant is fixed, if overshoot O_s occurs, certain amount of time is required for the velocity to achieve convergence and therefore operability is deteriorated during this period. Then, in order to avoid overshoot, ζ_i $(i = x, y, m)$ is chosen as ζ_x = 1, ζ_y = 1, ζ_m = 1. In addition, T_x = 0.4, T_y = 0.4 and T_m = 0.4, is used.

On the other hand, in the case of second order controller, ω_n is determined such that the system is not influenced by the noise included in the input and good operability of OMW is also obtained. Then, in this case, (ω_n) is chosen, by trial and error, as $(\omega_n)_x$ = 4, $(\omega_n)_y$ = 4, $(\omega_n)_m$ = 4.

Experimental comparison of the jerk produced in *x* direction by a first order controller and a second order controller, for the same reference velocity, was conducted. The experimental parameters were: K_x = 0.02, T_x = 0.4, ζ_x = 1.0, $(\omega_n)_x$ = 4.0, sampling time t_s = 0.03[s]. OMW was moved in automatic mode with an input help force given as:

$$f_x = \begin{cases} 0 & (0 \le t < 1, 4 \le t < 7, t \ge 10) \\ 50 & (1 \le t < 4) \\ -50 & (7 \le t < 10) \end{cases}$$

Jerk was evaluated by differentiating the output of the encoders of OMW's motors. Experimental results are shown in Fig. 2. v_x is the reference velocity, j_x^{omw}

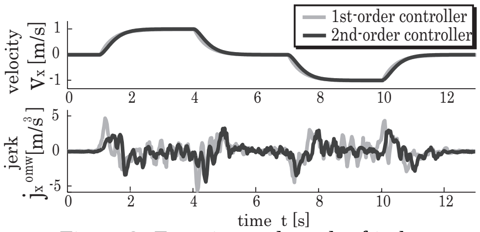

Figure 2: Experimental result of jerk.

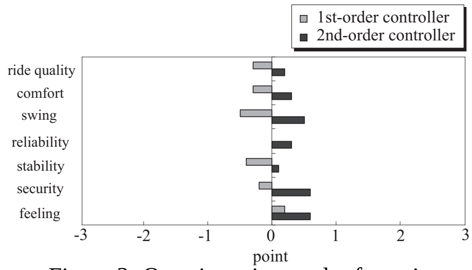

Figure 3: Questionnaire result of x-axis.

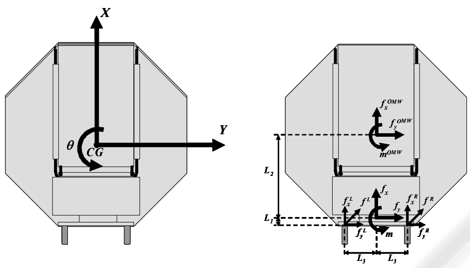
(a) Coordinate system of the OMW. (b) Decomposition of the forces applied to the handles of the OMW.

Figure 4: Working force.

shows the actual jerk that was calculated by using the encoders output.

In addition, as riding comfort is something that depends on the subjective judgement of the OMW's occupant, riding comfort was evaluated by using Semantic Differential (SD) method. The mean value of the results obtained in each item of the SD questionnaire are shown in Fig. 3 for *x* direction. It is possible to see that the values obtained by the second order controller are much better than that obtained by the first order controller. Then a second order controller will be used as power assist controller because it can improve riding comfort.

3.2 Direction Estimator of Navigation for Input Force

When the user tries to rotate OMW around its gravity center, OMW begins to slide and the radius of rotation sometimes becomes very big. Then, rotation around the center is very difficult (Kitagawa et al., 2004). A survey was conducted among various attendants trying to discover some relationships in the way they realized forwards-backwards, lateral and rotational movements. The goal of the survey was to find general rules that related the three mentioned motions. Even when it was impossible to find general rules that explained all cases, a relationship was found between lateral and rotational movements. These relationships were used as the base for constructing a fuzzy reasoning system (MathWorks, 2002)-(Harris et al., 1993) that helped to improve the operability of the OMW. These rules, in which just lateral motion and rotational motion are considered, are shown in Table 1. The block diagram of the system that considers power assist and fuzzy reasoning is shown in Fig. 5.

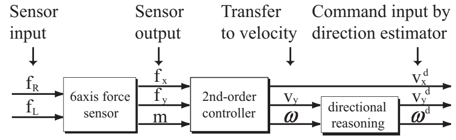

Figure 5: Block diagram of power assist system.

Table 1: Fuzzy reasoning rules.

Rule	Antecedent	Consequent
1	$v_y > 0$ and $\omega < 0$,	$v_y^d > 0$ (Right Slide)
2	$v_y < 0$ and $\omega > 0$,	$v_y^d < 0$ (Left Slide)
3	$v_y \approx 0$ and $\omega \approx 0$,	$v_y^d \approx 0$ (Not Slide)
4	$v_y \geq 0$ and $\omega > 0$,	$\omega^d > 0$ (CCW Turn)
5	$v_y \leq 0$ and $\omega < 0$,	$\omega^d < 0$ (CW Turn)
6	$v_y \approx 0$ and $\omega \approx 0$,	$\omega^d \approx 0$ (Not Turn)

In order to establish the rules of direction inference, first, the force applied to the grips of the force sensor are changed to the center of OMW, as shown in Fig. 4. Note that the input of the direction estimator is velocity V_{omw}, not force F. It may seem more reasonable to use F for the estimation of the attendant's intention, however, it is very difficult to derive transform equations from F, because of an effect of vibration of input force or noise. v_x is not included since forward and backward motion can be realized without direction estimation. Features of slide motion is expressed by Rules 1 and 2 in Table 1, and that of rotation by Rules 4 and 5. Rules 3 and 6 are added not to generate the reference velocity when input velocity is zero. The reason of these rules is shown in Table 1. Table 1 is described in detail in (Kitagawa et al., 2004), and hence the explanation is omitted due to the paper space.

Figure 6 shows the graph of membership functions of the first rule. The membership function of the antecedent of 1, 2, 4 and 5 is

$$\mu_{name} = \tan^{-1}\{a_{name}(\beta_i - b_{name})\}/\pi + 0.5, \quad (2)$$

where β_i is input ($\beta_1 = v_y$, $\beta_2 = \omega$) and a_{name} and b_{name} are tuning parameters. '$name$' is replaced by the name of each membership function. The first letter of 'name' of antecedents indicates sensor output(v_y^d:Y, ω^d:O), the second letter indicates sign

Table 2: Parameters of menbership functions.

Rule Number	Antecedent			
	name	a	b	c
1	YPS	7	0.3	-
	ONS	7	-0.3	-
2	YNS	7	-0.3	-
	OPS	7	0.3	-
3	YZS	-	-	1000
	OZS	-	-	1000
4	YPT	7	0.3	-
	OPT	7	0.3	-
5	YNT	7	-0.3	-
	ONT	7	-0.3	-
6	YZT	-	-	1000
	OZT	-	-	1000

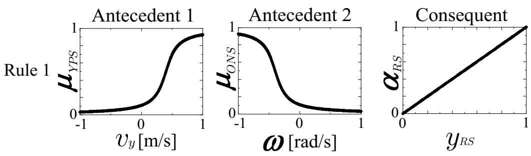

Figure 6: Membership functions of rule 1.

(Positive:P, Negative:N, Zero:Z), and the third letter indicates the realized motion (Slide:S, Turn:T).

The membership function of the antecedent of 3 and 6 is

$$\mu_{name} = \exp(-c_{name} \cdot \beta_i^2), \qquad (3)$$

where c_{name} is a tuning parameter.

3.3 Experimental Results

In order to verify the effectiveness of the control system, laboratory experiments were conducted. The results shown correspond to a first order controller. Parameters of the membership function of Fig. 6 are shown in Table 2. These parameters are given by trial and error method. The details are described in the former paper (Kitagawa et al., 2004).

The trajectory and velocity v_{omw}^d of slide motion to right are shown in Fig. 7 and Fig. 8, respectively. As seen in the trajectory of v_y^d, vibration of the velocity was reduced. The trajectory and velocity v_{omw}^d of rotation around its center in counter-clockwise are shown in Fig. 9 and Fig. 10, respectively. As seen in Fig. 9, the rotation around its center was realized by using the direction estimator. The effectiveness of the direction estimator is shown especially in case of rotation. In this case, the gain of the controller for the velocity in the direction X, **Vx**, was reduced to very small value in order to tes the goodness of the approach.

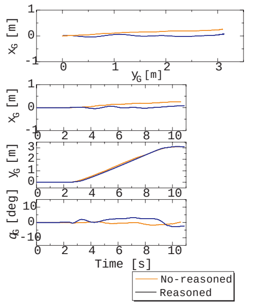

Figure 7: Trajectory of right slide.

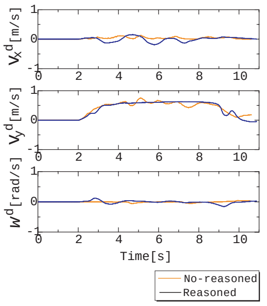

Figure 8: Velocity v_{omw}^d of right slide.

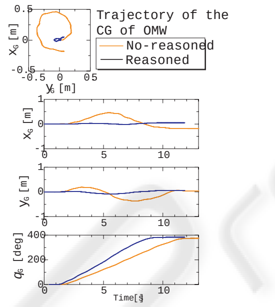

Figure 9: Trajectory of rotation (CCW).

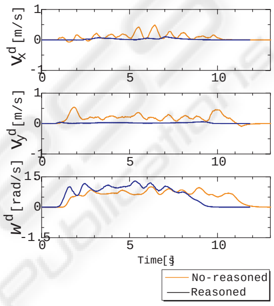

Figure 10: Velocity v_{omw}^d of rotation (CCW).

4 TUNING OF FUZZY SYSTEM

Figure 11 shows attendant's intention representing direction to make OMW move using v_y and ω added by attendant. In the present fuzzy parameters given by the previous section, the attendant such as *examinee 1* can operate OMW well. On the other hand, the attendant such as *examinee 2* wants to make OMW move towards right in the region of $v_y > 0$ and $\omega \approx 0$.

Then, when fuzzy membership function is fixed based on *examinee 1* for all examinees, the attendant with having the tendency like *examinee 2* feels the difficulty to operate OMW. Therefore, it is necessary to adjust the parameters of fuzzy membership functions according to the driving characteristics of individual attendants.

The fuzzy system must be tuned to respond to the particular characteristics of each attendant. As the tuning by trial and error is a time consuming and certainly not optimal, the tuning of the fuzzy system by using a neuro-fuzzy system is proposed in this paper. In the literature there are many neuro-fuzzy systems. ANFIS(Adaptive-Network-Based Fuzzy Inference System) (Jang, 1993) was chosen for this research. The details of the implementation of ANFIS are not presented here. For further information refer to (Jang, 1993).

According to the rules shown in Table 1, the range

Table 3: Fuzzy rules for ANFIS.

R	Antecedent	Consequent
1	If V_N and ω_N,	$y_1 = A_1 \times V_N + B_1 \times \omega_N + C_1$
2	If V_Z and ω_N,	$y_2 = A_2 \times V_Z + B_2 \times \omega_N + C_2$
3	If V_P and ω_N,	$y_3 = A_3 \times V_P + B_3 \times \omega_N + C_3$
4	If V_N and ω_Z,	$y_4 = A_4 \times V_N + B_4 \times \omega_Z + C_4$
5	If V_Z and ω_Z,	$y_5 = A_5 \times V_Z + B_5 \times \omega_Z + C_5$
6	If V_P and ω_Z,	$y_6 = A_6 \times V_P + B_6 \times \omega_Z + C_6$
7	If V_N and ω_P,	$y_7 = A_7 \times V_N + B_7 \times \omega_P + C_7$
8	If V_Z and ω_P,	$y_8 = A_8 \times V_Z + B_8 \times \omega_P + C_8$
9	If V_P and ω_P,	$y_9 = A_9 \times V_P + B_9 \times \omega_P + C_9$

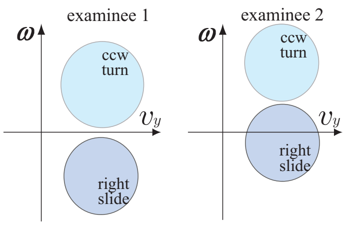

Figure 11: Attendant's intention.

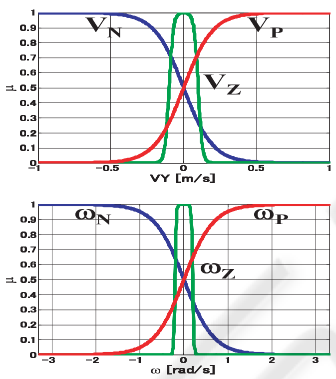

Figure 12: Partition of the ranges of V_y and ω.

of V_y and ω is divided in three Membership Functions (MF), Negative (V_N and ω_N), Zero (V_Z and ω_Z) and Positive (V_P and ω_P), as shown in Fig. 12. The functions used for the partitions of the range of V_y and ω, shown in Fig. 12, are called the $dsigmoidal$ (MathWorks, 2002) functions, and are defined as the difference of two sigmoidal functions. That is, if Eq. (4) is a sigmoidal function, with parameters a and c,

$$f(x,a,c) = \frac{1}{1+e^{-a(x-c)}} \quad (4)$$

A $dsigmoidal$ function can be defined as

$$f(x,a_1,c_1)-f(x,a_2,c_2)=f(x,[a_1,c_1,a_2,c_2]) \quad (5)$$

As there are 6 membership functions, and each with 4 parameters, there must be 24 parameters that are denoted as ($a_1 ... a_{12}$), ($c_1 ... c_{12}$).

Then, as there are three partitions in each variable, the total number of rules must be 3 × 3 = 9 rules,

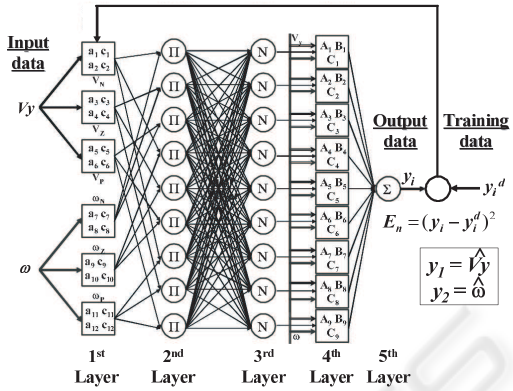

Figure 13: ANFIS system.

which are shown in Table 3. The odd rules correspond to those shown in Table 1, while the even rules are used for completeness. In the rules shown in Table 3 the consequents are a function of the inputs because a Takagi-Sugeno-Kang (TSK) (Takagi and Sugeno, 1985) system is being used, instead of the Mamdani (Mamdani and Assilian, 1985) system used for the rules of Table 1. The coefficients of the consequents are denoted by ($A_1 ... A_9$), ($B_1 ... B_9$) and ($C_1 ... C_9$), as shown in Table 3. The ANFIS equivalent of this system is shown in Fig. 13. ANFIS has 5 layers:

- ***1st Layer:*** Here the inputs **Vy** and ω are subjected to the action of the membership functions of Fig. 12, that are represented by its parameters (a_1 ... a_{12}) and (c_1 ... c_{12}).
- ***2nd Layer:*** In the 2nd Layer the fuzzy rules shown in Table 3 are constracted. As the antencedents are jointed by a logic "AND", this relationship is mathematically obtained by the product (Π) of the two antecedents. The output of each node represents the firing strength of a rule, that is represented by ω_i (i = 1 ... 9).
- ***3rd Layer:*** This is a normalization layer, where the ratio of the i^{th} rules' firing strength to the sum of all rules firing strength is calculated.
- ***4th Layer:*** Here the normalized firing strength that comes from the 3rd Layer is multiplied by the output functions of the fuzzy reasoning system.
- ***5th Layer:*** The overall output of the system is computed as the sum of all the incoming signals.

For using ANFIS, the structure of the block labeled as "directional reasoning" in Fig. 5 is shown in Fig. 14. It is clear that two fuzzy systems, one for **Vy**, and the other for ω are used.

For the off-line training of ANFIS system of the OMW, the following approach was followed:

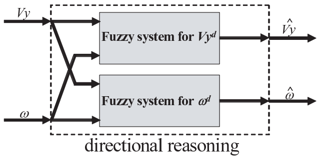

Figure 14: Contents of the block ***directional reasoning***.

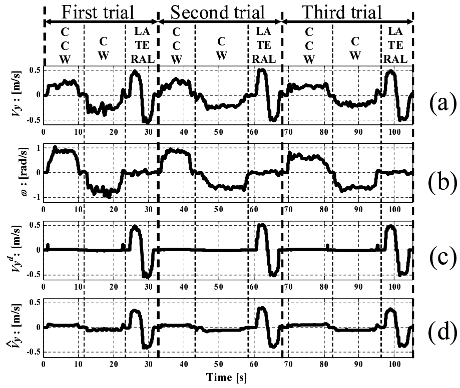

Figure 15: Input data and results of teaching for the case of lateral movement((a)-(b): input data, (c): teaching data and (d): estimated output data).

(i) An attendant is asked to conduct five kind of movements composed of: (1) forward and backward movement, (2) lateral movement, (3) counter-clockwise (CCW) rotation, (4) clockwise (CW) rotation and (5) forwards and backwards diagonal movement, for five times. For taking this data just power assistance is used. Three groups of data will be used for the training of ANFIS and the remaining two for the testing of the obtained results.

(ii) ANFIS is trained and tested by using a simulation program developed in Matlab. The validity of this simulator has been tested by comparing the results obtained from simulation and experiments.

(iii) The obtained parameters are saved in the computer of the OMW and the system is tested by experiments.

In this paper, the simulation results will correspond to one attendant called **"Attendant 1"**. Fig. 15 shows the input data (a)-(b), the teaching data (c), and the estimated output data (d) after the training by ANFIS for **"Attendant 1"** for the case of lateral movement. In Fig. 16 the same information is shown for the case of rotational movement. The teaching data was constructed following the logic of Table 3. The ANFIS systems was trained by using the input and teaching data shown in Fig. 15 and Fig. 16. The total error in each epoch was calculated as:

$$J = \Sigma_{n=1}^{N} E_n, \qquad (6)$$

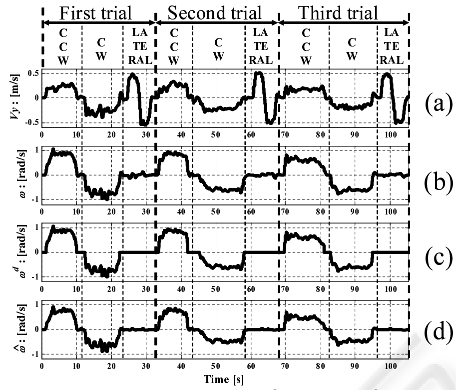

Figure 16: Input data and results of teaching for the case of rotational movement((a)-(b): input data, (c): teaching data and (d): estimated output data).

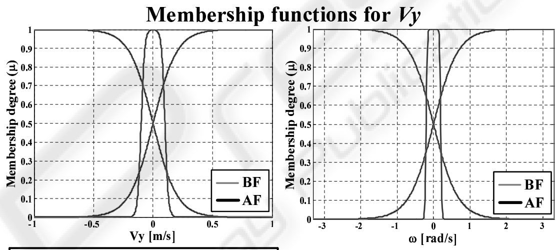

Output Coefficients					
A		B		C	
BF	AT	BF	AT	BF	AT
0	-1.28	0	0.17	0	-0.34
0	-0.36	0	0.59	0	0.36
1	-3.32	0	-1.64	0	-0.58
1	3.76	0	-0.20	0	0.35
0	-1.62	0	0.18	0	-0.01
1	3.74	0	-0.47	0	-0.33
1	-2.40	0	0.16	0	-0.41
0	-0.08	0	0.46	0	-0.33
0	-0.15	0	-1.27	0	1.24

BF: Before training
AT: After training

Figure 17: Results of training of ***Vy*** system.

where,

$$E_n = (y_i(n) - y_i^d(n))^2, \qquad (7)$$

with n being the n^{th} data and N the total number of data used for the training. Tuning is performed by minimizing the output error of the NN used in combination with the fuzzy inference system. For achieving this goal, the NN is trained by using a hybrid method that combines least squares and the Backpropagation algorithm (BP law). This method is thus thought to be an effective method for tuning the parameters of the OMW's fuzzy inference system. In the case shown in Fig. 15 and Fig. 16, N = 8530. According to the results obtained from different trials, it has been found that, in order not to lose the generality, the miminum total error allowed should be around 0.05 for both systems. The time needed for the training of the ANFIS system is around 1 [min], and the convergence to the desired values of error is reached after 20 epochs. The results of the training are shown in Fig. 17 and Fig. 18. It is possible to note that the shape of the member-

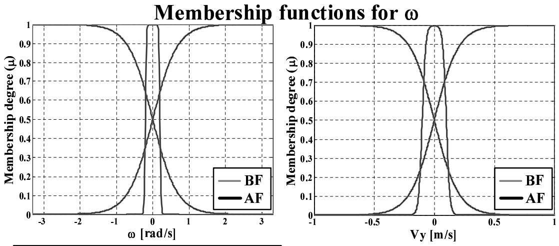

Output Coefficients					
A		B		C	
BF	AT	BF	AT	BF	AT
0	0.88	1	1.56	0	0.92
0	-0.55	1	-0.79	0	-1.49
0	5.65	0	3.47	0	1.67
0	-1.21	0	-0.61	0	-0.19
0	0.13	0	-1.87	0	-0.02
0	-2.22	0	0.68	0	0.22
0	1.24	0	1.72	0	-0.66
0	0.11	1	-0.99	0	1.47
0	-1.91	1	3.70	0	-1.90

BF: Before training
AT: After training

Figure 18: Results of training of ω system.

ship functions almost does not change for any of the systems, ***Vy*** or ω. However, the change in the output function is easily seen. By the change in the output functions the system adjust to the input data of the attendant.

Results for one case of testing data, that the training of ANFIS did not include, are shown in Fig. 19. The trajectory of the OMW when **"Attendant 1"** rotates the OMW in CCW direction and moves the OMW in lateral direction by using just power assist, are shown in Fig. 19 (a) and Fig. 19 (b). It is possible to see that CCW rotation is influenced by the lateral velocity and the velocity in direction **X**. The lateral movement is almost a perfect horizontal line. Fig. 19 (c) and Fig. 19 (d) show the result for CCW rotation and lateral movement after ANFIS was applied. As lateral movement is almost the same as desired, from now the discussion will be centered in the rotational movement in CCW direction. As expected from the results shown in Fig. 16 the rotational movement in CCW direction has been improved by reduction of the lateral velocity. However, as in this case the gain of the controller for **Vx** has not been reduced as it happened in the cases shown in Fig. 7 - Fig. 10, there is some displacement in direction **X**. Just reducing the gain of the controller in the direction **X**, as before, could be a good solution. However, it will influence the movement of the OMW when the attendant wants to easily move forwards or backwards. Then, some relationship must be established between the different movements studied here: rotation, lateral and forwards and backwards, that allows to reduce the velocity in direction **X**, ***Vx***, when rotating and let it pass almost untouched when moving forwards or backwards. The influence of ***Vx*** in the lateral movement is almost irrelevant, and for that reason is not considered any action in the case of lateral movement.

After the reasoning system has been trained with

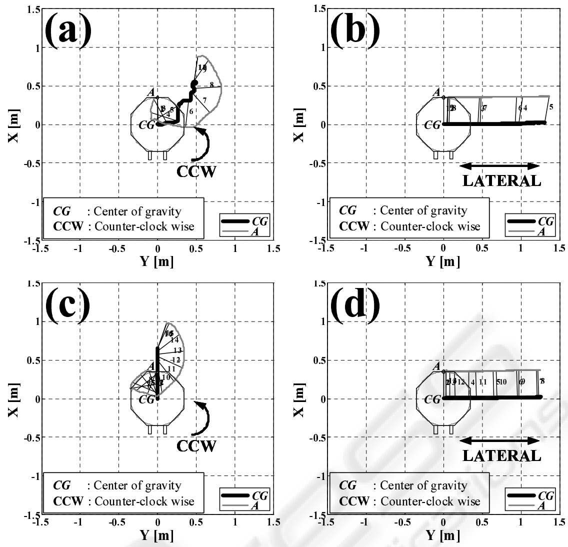

Figure 19: Trajectory of the OMW in CCW rotation and lateral movement. (a) and (b) show the cases in which power assist only is used, and (c) and (d) the result by ANFIS.

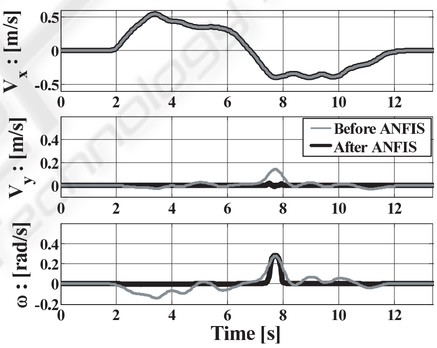

Figure 20: **Vx**, **Vy** and ω for a case of forwards and backwards movement of the OMW, by**"Attendant 1"**.

ANFIS, in the case when the movement of the OMW is not a rotational movement, ω is reduced according to the training described in previous paragraphs. It happens in the case of lateral movement and in the case of forwards and backwards movement too. By studying the value of ω when **"Attendant 1"** moves the OMW forwards and backwards, it has been found that it is always less than 0.3 [rad/s]. Fig. 20 shows one case of forwards and backwards movement. Establishing a rule in which for all the cases in which ω is less than 0.3 [rad/s] was considered in principle. However it will ignore cases like the one shown in Fig. 21.

In Fig. 21 it is possible to see that for a rotational movement the value of ω is greater than 0.2 [rad/s] and it happens in all the cases studied for **"Attendant 1"**. Then a rule is established such as **Vx** must be multiplied by a Reducing Multiplicative Factor (RMF) if the value of ω is greater than 0.2 [rad/s]. The value

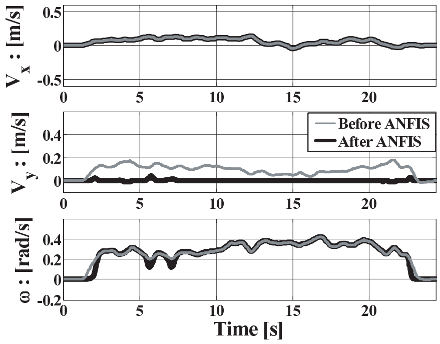

Figure 21: **Vx**, **Vy** and ω for a case of rotational movement of the OMW, by **"Attendant 1"**.

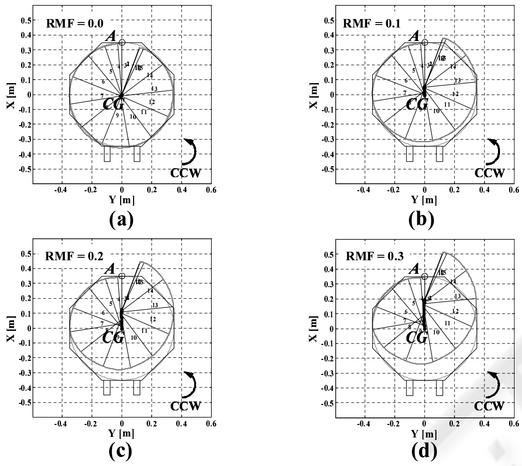

Figure 22: Trajectory of the OMW in CCW rotation when the Reduction Multiplicative Factor (RMF) is (a) RMF = 0, (b) RMF = 0.1, (c) RMF = 0.2 and (d) RMF = 0.3.

of RMF is decided by trial and error, by trying multiples of 0.1. Fig. 22 shows the cases in which RMF = 0, 0.1, 0.2, 0.3. As it is seen there, a value greater than 0.2 is not so good. Then it is decided that the range of variation of RMF must be [0 $\sim$ 0.2], and the mean value, 0.1, is chosen for this research. Results the reduction of Vx are shown in Fig. 23 for CCW rotation, lateral movement and forwards and backwards movement, when RMF = 0.1. It is possible to see that operability has been improved by the application of the fuzzy reasoning system tuned by ANFIS. In this paper, the threshold of ω is 0.2 [rad/s] and RMF = 0.1. But these values may change by attendant. Therefore, it is a future problem to generalize how to determine these values such as RMF and threshold.

5 CONCLUSIONS

A power assist system for omni-directional wheelchairs considering both attendant's manipulability

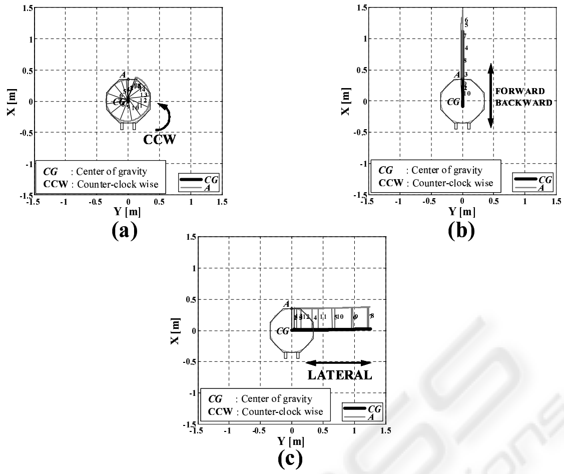

Figure 23: Improvement of the trajectory of the OMW in CCW rotation when **Vx** is multiplied by a factor 0.1.

and rider's comfort has been developed. The reference velocity of the omni-directional wheelchair was derived from attendant's input force. Operability of rotation was improved greatly by using the fuzzy direction estimator. The membership functions of the fuzzy systems are tuned using attendant's input data by applying a neuro-fuzzy system (ANFIS).

ACKNOWLEDGEMENTS

This work was partially supported by The 21^{st} Century COE (Center of Excellence) Program "Intelligent Human Sensing"

REFERENCES

FrankMobilitySystems (2002). Frank mobility systems inc. In *http://www.frankmobility.com/*.

Harris, C. J. et al. (1993). Intelligent control. World Scientific.

Jang, J. (1993). Anfis: Adaptive-network-based fuzzy inference system. In *IEEE Transactions on Systems, Man, and Cybernetics, Vol. 23(3), pp. 665-685*.

Kitagawa, H. et al. (2001). Semi-autonomous obstacle avoidance of omnidirectional wheelchair by joystick impedance control. In *Proc. IEEE/RSJ Int. Symp. on Intelligent Robots and Systems, pp. 2148-2153*.

Kitagawa, H. et al. (2002). Motion control of omnidirectional wheelchair considering patient comfort. In *Proc. IFAC World Congress, T-Tu-E20*.

Kitagawa, H. et al. (2004). Fuzzy power assist control system for omni-directional transport wheelchair. In *Proc. IEEE/RSJ Int. Conf. on Intelligent Robots and SystemsC1580-1585*.

Lin, C. T. and Lee, C. S. G. (1991). Neural-network-based fuzzy logic control and decision system. In *IEEE Trans. on Computers, Vol. 40(12), pp. 1321-1336*.

Maeda, H. et al. (2000). Development of omni-directional cart with power assist system (in japanese). In *Proc. 18th Annual Conf. of Robotics Society of Japan, 15, pp.1155-1156*.

Mamdani, E. H. and Assilian, S. (1985). An experiment in linguistic synthesis with a fuzzy logic controller. In *International Journal of Man-Machine Studies, Vol. 7(1), pp. 1-13*.

MathWorks (2002). Fuzzy logic toolbox user's guide version 2, pp. 3-18. The Matworks Inc.

Seki, H. et al. (2005). Novel driving control of power assisted wheelchair based on minimum jerk trajectory. In *IEEJ Trans. EIS Vol. 125(7) (in Japanese), pp. 1133 - 1139*.

Takagi, T. and Sugeno, M. (1985). Fuzzy identification of systems and its applications to modeling and control. In *IEEE Transactions on Systems, Man and Cybernetics, Vol. 15(1), pp. 116 - 132*.

Terashima, K. et al. (2004). Frequency shape control of omni-directional wheelchair to increase user's comfort. In *Proceedings of the 2004 IEEE International Conference on Robotics and Automation (ICRA), pp. 3119-3124*.

Wada, M. and Asada, H. (1999). Design and control of a variable footprint mechanism for holonomic omnidirectional vehicles and its application to wheelchairs. In *Proc. IEEE Trans. Robot. Automat, 15, pp. 978-989*.

West, M. and Asada, H. (1992). Design of a holonomic omnidirectional vehicle. In *Proc. IEEE Int. Conf. Robot. Automat., pp. 97-103*.

SciTePress Science and Technology Publications